Journal of Statistical Mechanics:
Theory and Experiment

SISSA

STATPHYS 27

Brownian motion and beyond: first-passage, power spectrum, non-Gaussianity, and anomalous diffusion

To cite this article: Ralf Metzler *J. Stat. Mech.* (2019) 114003

View the article online for updates and enhancements.

IOP ebooks™

Bringing you innovative digital publishing with leading voices to create your essential collection of books in STEM research.

Start exploring the collection - download the first chapter of every title for free.

This content was downloaded from IP address 129.187.254.46 on 07/11/2019 at 18:11

Journal of Statistical Mechanics: Theory and Experiment
An IOP and SISSA journal

Brownian motion and beyond: first-passage, power spectrum, non-Gaussianity, and anomalous diffusion

Ralf Metzler

Institute of Physics and Astronomy, University of Potsdam, 14476 Potsdam-Golm, Germany
E-mail: rmetzler@uni-potsdam.de

Received 20 August 2019
Accepted for publication 25 September 2019
Published 1 November 2019

Online at stacks.iop.org/JSTAT/2019/114003
https://doi.org/10.1088/1742-5468/ab4988

Abstract. Brownian motion is a ubiquitous physical phenomenon across the sciences. After its discovery by Brown and intensive study since the first half of the 20th century, many different aspects of Brownian motion and stochastic processes in general have been addressed in Statistical Physics. In particular, there now exists a very large range of applications of stochastic processes in various disciplines. Here we provide a summary of some of the recent developments in the field of stochastic processes, highlighting both the experimental findings and theoretical frameworks.

Keywords: Brownian motion, diffusion

J. Stat. Mech. (2019) 114003

© 2019 IOP Publishing Ltd and SISSA Medialab srl

1742-5468/19/114003+18$33.00

Contents

1. Introduction

In his seminal account Robert Brown reported the seemingly erratic motion of granules of 1/4000 to 1/5000 of an inch in size, extracted from pollen grains of the plant Clarkia pulchella. Being a botanist, Brown then went on to prove that the observed jiggling motion is not due to the active motion of 'animalcules'. Detecting the same type of motion of small granules of inorganic matter—such as granite or a piece of the Egyptian Sphinx—he demonstrated that the diffusive particle motion is in fact a true physical phenomenon [1]. The precise understanding of Brownian motion was then established in the groundbreaking works of Albert Einstein [2], William Sutherland [3], Marian Smoluchowski [4], and Paul Langevin [5]. Based on different arguments, they derived the linear time dependence of the mean squared displacement (MSD)

$$\langle \mathrm{r}^2(t)\rangle = \int \mathbf{r}^2 P(\mathbf{r},t)\mathrm{d}V = 2dDt \tag{1}$$

in d spatial dimensions, and the Gaussian nature of the probability density function (PDF) for a δ-initial condition (Green's function)

$$P(\mathbf{r},t) = \frac{1}{(4\pi Dt)^{d/2}} \exp\left(-\frac{\mathbf{r}^2}{4Dt}\right). \tag{2}$$

This Gaussianity of $P(\mathbf{r},t)$ was independently established in the discussion of the 'random walk' in an exchange between Karl Pearson and John William Strutt, third Lord Rayleigh [6].

The theoretical foundation of diffusion, especially the connection of the diffusion coefficient D with thermal energy $k_\mathrm{B}T$ and thus Avogadro's number N_A in the Einstein–Smoluchowski–Sutherland relation

$$D = \frac{k_\mathrm{B}T}{m\eta} = \frac{(R/N_\mathrm{A})T}{m\eta} \tag{3}$$

J. Stat. Mech. (2019) 114003

in terms of the test particle mass m, the viscosity η of the ambient fluid, and the gas constant R, prompted a long series of ever improving experiments on diffusive motion. Jean Perrin's systematic observations of microscopic diffusing particles were groundbreaking in the introduction of single particle tracking protocols [7]. Additional noteworthy contributions were due to Ivar Nordlund, who introduced time-resolved recordings using a moving film plate and thus getting around the need to average over—often not fully identical—ensembles of test particles [8], and Eugen Kappler, who studied the torsional diffusion of a small mirror suspended on a long, thin quartz thread [9]. In fact, as this mirror experienced a restoring force by the twisting thread—to first order, a Hookean force—it was Kappler who first mapped out the Gaussian Boltzmann distribution of the equilibrium distribution of the angles, to very high precision.

Today, following massive advances in microscopic techniques such as superresolution microscopy (2014 Nobel Prize to Eric Betzig, William Moerner, and Stefan Hell) it is possible to follow submicron tracer particles or even fluorescently labelled single molecules in highly complex environments such as living biological cells [10, 11]. Thus, spatial resolutions in the range of a few nanometres and time resolutions in the microsecond range have been achieved [12]. Concurrently, supercomputing methods based on molecular dynamics (2013 Nobel Prize to Arieh Warshel, Michael Levitt, and Martin Karplus) have vastly improved, and huge data sets on complex systems such as crowded lipid membranes are routinely produced [13].

The high spatiotemporal resolution of measured or simulated diffusive motion in often complex environments have prompted numerous new developments in the theoretical description of stochastic processes. Among these are new results on Brownian first-passage dynamics, particularly, resolving the full density of first-passage times. On a fundamental statistical physics level are questions on ergodicity and reproducibility pinpointing whether the long time average of single particle motion converges to the behaviour of an ensemble of identical particles, or under what conditions repeated measurements can be expected to deliver practically the same results. At finite measurement times, the time averages of physical observables fluctuate from realisation to realisation, and the quantification of these fluctuations allows one to extract information on the system. Another feature observed in a growing number of experiments is the non-Gaussianity of the PDF, and models to describe this behaviour are called for. Finally, we mention anomalous diffusion, in which the MSD no longer has the linear time dependence (1). In what follows we highlight briefly these new developments. Section 2 addresses first-passage processes beyond mean values, relevant in search and reaction processes. In section 3 we discuss the quantification of single particle trajectories, in particular, in terms of single trajectory power spectra. Section 4 addresses the phenomenon of non-Gaussian diffusion and its theoretical description. In section 5 we conclude and present a perspective.

2. First-passage times: beyond mere means

Consider a diffusing particle in one dimension that is initially released at position $x_0 > 0$ at time $t = 0$ on the half-line $x > 0$ and with an absorbing boundary at the origin. Solving

J. Stat. Mech. (2019) 114003

the boundary value problem produces the survival probability $\mathscr{S}(t) = \int_0^\infty P(x,t)\mathrm{d}x$. Its negative derivative is the first-passage time density [14]

$$\wp(t) = -\frac{\mathrm{d}\mathscr{S}(t)}{\mathrm{d}t} = \frac{x_0}{(4\pi Dt)^{3/2}} \exp\left(-\frac{x_0^2}{4Dt}\right), \tag{4}$$

which is a one-sided probability density function of Lévy–Smirnov type. At short times the first-passage time PDF has an exponential cutoff $\propto t^{-3/2}\exp(-x_0^2/[4Dt])$, reflecting the fact that the particle needs a finite time to move from x_0 to the origin. The long-time behaviour is given by the power-law $\wp(t) \simeq t^{-3/2}$, causing the divergence of the mean first-passage time $\langle t\rangle$. Note that this 3/2 power-law asymptote based on Sparre Anderson's result [14] is universal for all Markovian symmetric random walks, in particular, with power-law jump length distributions [14, 15]. Once the first-passage process runs off in a finite domain—in higher dimensions, with a finite-size target—the mean first-passage time $\langle t\rangle$ remains finite. Remarkably, even for the mean first-passage time—or its 'global' value, averaged over all possible initial conditions—a number of novel, high-profile results have been reported in recent years [16], underlining that the mathematical development of first-passage processes is far from complete.

The point we want to stress here is that the situation becomes even more subtle when we go beyond the (global) mean first-passage time and consider the full PDF of first-passage times in a finite domain. A first indication that such a study is relevant comes from the observation that in typical settings the times of two independent realisations of first-passage events are disparate. In other words, the distributions of the 'uniformity index' $\omega = \frac{t_1}{t_1+t_2}$ of two first-passage times t_1 and t_2—with the same initial condition in the same system—are effectively broad [17]. On a more applied level, for biochemical reactions in living cells, where the relevant molecules often occur at minute, nanomolar concentrations, it is relevant to have information on the diffusive reaction control beyond global mean first-passage times, and the associated triggering reactions have a clear dependence on the initial distance between the release of the particle and its designated binding spot [18]. As our discussion below shows, this property is beyond the concept of the mean first-passage time. Indeed, distributions of first-passage times in this cellular context were shown to become broad [19]. Experimentally, it is already possible to resolve the production event of a single protein in a living cell [20], and it was shown that even relatively small, green fluorescent proteins can be traced in live cells [12]. It will be possible to follow individual biomolecules in their natural environment and determine the molecule-resolved first-passage times in the foreseeable future.

To quantify more precisely how broad the distribution of first-passage times in a finite domain becomes, a Newton series technique for the calculations of $\wp(t)$ for a range of different diffusion processes and spatial dimensions was developed in hyperspherical domains [21]. In all cases the PDF of first-passage times features distinct regions: (i) an exponential suppression at very short times combined with a global maximum, analogous to the behaviour captured in the Lévy–Smirnov type PDF (4). The maximum value occurs at the point taken by 'direct' trajectories, that move relatively straight from the initial point to the target. This is what may be called 'geometry-control'. (ii) The second region is given by a power-law decay with a process-dependent scaling exponent. (iii) In the long time limit an exponential shoulder occurs whose characteristic time depends both on the specific process and the details of the diffusive domain.

J. Stat. Mech. (2019) 114003

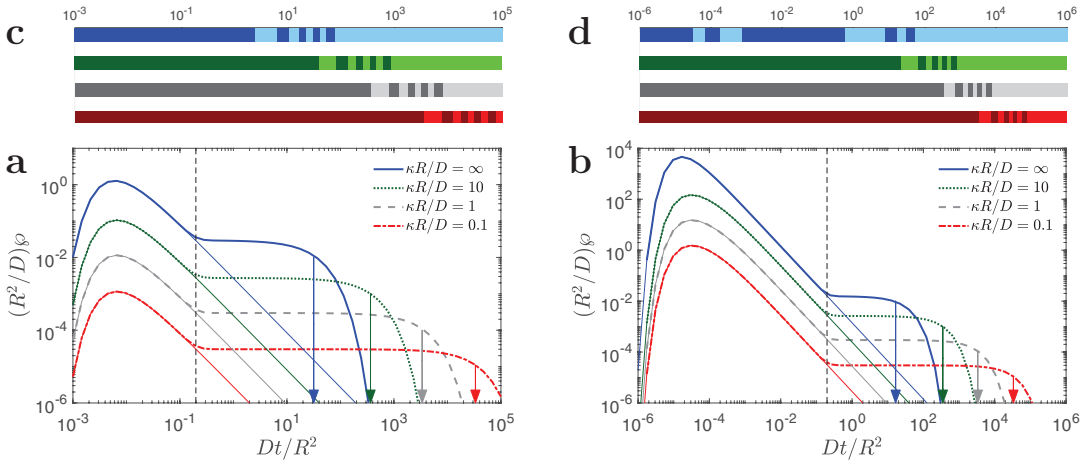

Figure 1. Reaction time density $\wp(t)$ for a reaction on an inner target of radius $\rho/R = 0.01$, with starting point (a) $r/R = 0.2$ and (b) $r/R = 0.02$ for four progressively decreasing (from top to bottom) values of the dimensionless reactivity $\kappa R/D$ defined in the plot. The coloured vertical arrows indicate the mean reaction times for these cases. The vertical black dashed line indicates the crossover time $t_c = 2(R-\rho)2/(D\pi^2)$ above which the contribution of higher order eigenmodes becomes negligible. This characteristic time marks the end of the hump-like region (Lévy–Smirnov region specific to an unbounded system) and indicates the crossover to the plateau region with equiprobable realisations of the reaction times. The plateau region spans a considerable window of reaction times, especially for lower reactivity values. Thin coloured lines show the reaction time for the unbounded case ($R \to \infty$). Length and time units are fixed by setting $R = 1$ and $R^2/D = 1$. Note the extremely broad range of relevant reaction times (the horizontal axis) spanning over 12 orders of magnitude for panel (b). Coloured bar-codes (c) and (d) indicate the cumulative depths corresponding to the four considered values of $\kappa R/D$ in decreasing order from top to bottom. Each bar-code is split into ten regions of alternating brightness, representing ten 10%-quantiles of the distribution (e.g. the first dark blue region of the top bar-code in panel (c) indicates that 10% of reaction events occur until $Dt = R^2 \sim 1$.) Reproduced from [23]. CC BY 4.0.

This exponential regime corresponds to 'indirect' trajectories in which the diffusing particle strays off its path to the target and loses the memory to its initial condition due to collisions with the outer boundary of the domain. Notably, the characteristic time encoded in this exponential shoulder is closely related to the mean first-passage time. Looking at the numbers this means that measuring the mean first-passage time in such a process is in fact typically quite unlikely (see figure 1).

A somewhat more general situation was analysed in [22, 23], namely, when we combine the diffusing particle with a target of finite reactivity κ. For the mean reaction time, the contributions due to the diffusive motion (characterised by the diffusivity D) and the reaction (quantified by the reactivity κ), separate [23],

$$\langle t \rangle = \frac{(r-\rho)(2R^3 - \rho r(r+\rho))}{6Dr\rho} + \frac{R^3 - \rho^3}{3\kappa\rho^2} \tag{5}$$

J. Stat. Mech. (2019) 114003

for the case of a spherical domain with concentric target, where R is the outer (reflecting) radius, ρ is the radius of the partially reactive inner target, and r is the radius of initial release of the diffusing particle. The successful reaction in expression (5), which is analogous to the famed Collins–Kimball rate [24], thus requires the diffusive search from the point of release to the target (the 'diffusion control', inversely proportional to D) plus the time to overcome the 'reaction barrier' (the 'rate control', inversely proportional to κ).

The full first-passage time density to a successful reaction (or the 'reaction-time density') for this case is shown in figure 1. The features of the reaction-time density for a perfectly reactive target ($\kappa = \infty$) are identical to the above-described result for the first-passage in [21]. The initial exponential suppression and the most likely first-reaction time, as well as the intermediate power-law decay and the terminal exponential shoulder are in fact commonly shared for finite reactivity κ, as well. However, for decreasing reactivity the plateau region between the power-law and the terminal exponential decay becomes increasingly pronounced. In addition to the geometry-control in the most probable first-reaction time—whose value is the same for all cases, as this value corresponds to direct trajectories with immediate reaction success—the further defocusing of reaction-times at finite κ becomes more pronounced, the effect of 'reaction-control' [23]. Depending on the details, individual first-reaction times have a large probability to be shorter than the mean first-reaction time, as shown in the 'reaction depth' panels above the main graph in figure 1.

While in cases of macroscopic concentrations of reactive particles the mean reaction time (or its inverse, the chemical rate constant) is a meaningful quantity, at the minute concentrations in biochemical reactions, or in other 'first come first win' scenarios it loses its meaning, and a proper physical understanding of the process requires cognisance of the full distribution of first-passage or first-reaction times.

3. Single trajectory mean squared displacement

The most standard way to characterise a diffusion process is in terms of the MSD (1). For anomalous, non-Brownian diffusion, the MSD is often of the power-law form [25–27]

$$\langle \mathbf{r}^2(t) \rangle \simeq K_\alpha t^\alpha, \tag{6}$$

where according to the value of the anomalous diffusion exponent α we distinguish between subdiffusion ($0 < \alpha < 1$), Brownian diffusion ($\alpha = 1$), superdiffusion ($1 < \alpha < 2$), ballistic diffusion ($\alpha = 2$), and hyperdiffusion ($\alpha > 2$). Examples for subdiffusion include the classical charge carrier transport in amorphous semiconductors [28, 29], tracer diffusion in subsurface aquifers [30], or the motion of passive tracers in living biological cells [31]. Superdiffusion occurs in weakly chaotic or fully turbulent flows [32], or in actively driven motion in cells [33]. We note that sometimes, also higher order moments are being used, for instance, the skewness measuring the asymmetry of a PDF involves the third order moment, and the kurtosis providing information about the non-Gaussianity of a PDF is based on the fourth order moment, see the next section on

J. Stat. Mech. (2019) 114003

non-Gaussian distributions. Ratios of fourth order moments versus the squared second order moment were shown to distinguish different anomalous diffusion processes from another [34].

The MSD (1) or (6) are ensemble quantities, based on the evaluation of the second moment of the PDF $P(\mathbf{r},t)$. While this ensemble-averaged MSD is a good quantity when a large ensemble of particles are measured, in many modern setups such as single particle tracking, typically relatively few individual particle trajectories $\mathbf{r}(t)$ of finite length T are recorded. These are conventionally evaluated in terms of the time-averaged MSD [27, 35, 36]

$$\overline{\delta^2(t)} = \frac{1}{T-t}\int_0^{T-t}\Big[\mathbf{r}(t'+t)-\mathbf{r}(t')\Big]^2\mathrm{d}t'. \tag{7}$$

For an ergodic process, $\overline{\delta^2(t)}$ in the limit of long measurement times T will converge to the MSD: $\lim_{T\to\infty}\overline{\delta^2(t)} = \langle\mathbf{r}^2(t)\rangle$. This can be easily seen for a Brownian process, which is self-averaging over sufficiently long times. Thus, from a random walk perspective we say that the kernel in definition (7) is proportional to the number n of jumps in the time interval t, $[\mathbf{r}^2(t'+t)-\mathbf{r}^2(t')]^2 \sim 2dKt$, where $t = n\tau$ in terms of the number of jumps in the interval t and the time τ typically consumed for a single jump. Then the diffusion coefficient can be identified as $K = \sigma^2/(2d\tau)$, where σ^2 is the second moment of the jump length distribution [27, 35, 36]. Evaluating the integral in (7) then immediately produces that $\lim_{T\to\infty}\overline{\delta^2(t)} = 2dKt$, proving ergodicity. Note that for practical purposes in data analysis but also for calculations it is useful to define the mean time-averaged MSD over a set of N individual trajectories denoted by the index i [35, 36],

$$\left\langle\overline{\delta^2(t)}\right\rangle = \frac{1}{N}\sum_{n=1}^{N}\overline{\delta_i^2(t)}. \tag{8}$$

Anomalous diffusion is non-universal: there exist many different stochastic processes giving rise to the power-law form (6) of the MSD. The best known examples include continuous time random walks whose sojourn (trapping) times τ are power-law distributed, $\psi(\tau)\simeq\tau_0^\alpha/\tau^{1+\alpha}$ with $0<\alpha<1$, such that the characteristic sojourn time diverges [28]. Due to the lack of time scale, individual sojourn times may occur whose length is of the order of the duration of the process, no matter how long this process evolves. As a consequence, the time-averaged MSD behaves fundamentally differently from the ensemble MSD. Thus, while the MSD is of power-law form (6), the time-averaged MSD $\overline{\delta^2(t)}$ always remains a random quantity, even in the long measurement time limit [27, 35, 36]. Its mean can be shown to follow the relation ($t \ll T$) [35, 36]

$$\left\langle\overline{\delta^2(t)}\right\rangle \sim 2dK_\alpha\frac{t}{T^{1-\alpha}}. \tag{9}$$

The lag time (t) dependence is thus linear, as if the process were Brownian. The anomaly of the process can only be seen in the explicit dependence on the observation time T: the longer the process evolves, the more it slows down, reflecting the occurrence of ever longer waiting times, on average. This non-stationary behaviour is called ageing and is measured experimentally [37].

J. Stat. Mech. (2019) 114003

Ageing may also be relevant in a somewhat different setting: start a continuous time random walk process (or another ageing stochastic process) at some initial time, but commence the actual measurement at $t_a > 0$. The ageing time-averaged MSD reads [38]

$$\overline{\delta_a^2(t)} = \frac{1}{T-t}\int_{t_a}^{T+t_a-t}\left[\mathbf{r}(t'+t)-\mathbf{r}(t')\right]^2 \mathrm{d}t'. \tag{10}$$

For a continuous time random walk process with scale-free waiting times, the resulting behaviour is [38]

$$\left\langle\overline{\delta_a^2(t)}\right\rangle \simeq \Lambda_\alpha(t_a/T)\left\langle\overline{\delta^2(t)}\right\rangle, \quad \Lambda_a(z) = (1+z)^\alpha - z^\alpha. \tag{11}$$

Here the purely multiplicative factor Λ_α depends on the ratio t_a/T of the two time scales of the system, while on the right hand side of expression (11) the non-aged time-averaged MSD (7) appears. In the time average, that is, the ageing time t_a enters in a simpler way than in the corresponding ageing MSD, that exhibits a crossover behaviour from $\langle\mathbf{r}_a^2(t)\rangle \simeq t/t_a^{1-\alpha}$ for $t_a \gg t$ to $\simeq t^\alpha$ for $t \gg t_a$ [38, 39].

Non-ergodicity and ageing not only occur in scale-free continuous time random walks. While diffusion on the infinite cluster of a critical percolation network is ergodic, when we consider all clusters of a percolation network, due to the random seeding of the walkers on clusters of various sizes, non-ergodic behaviour results [40]. Other examples, in which the behaviours with respect to non-ergodicity and ageing have analogous expressions as relations (6), (9), and (11) are scaled Brownian motion defined in terms of a Markovian Langevin equation with time-dependent diffusion coefficient, $K(t) \simeq t^{\alpha-1}$ [41] as well as heterogeneous diffusion processes with position-dependent diffusivity $K(x) = K_0|x|^{2-2/\alpha}$ [42]. Ageing also affects other quantities of the associated process. For instance, it may induce a population splitting into mobile and immobile subpopulations: for scale-free continuous time random walks the probability that at least one jump occurs during the measurement period T decays with the ageing time t_a as $m_\alpha \simeq (T/t_a)^{1-\alpha}$ due to the increasing probability of ever larger sojourn times with growing t_a [38]. Similar effects occur in heterogeneous diffusion processes [43]. Another quantity that is directly affected by ageing is the first-passage time density [29, 44]. Conversely, ergodic anomalous diffusion processes exist in the form of processes driven by stationary but long-range correlated fractional Gaussian noise, namely, fractional Brownian motion [45, 46] and fractional Langevin equation motion [46, 47].

For finite-time measurements even a Brownian process will lead to non-identical results from one to the next trajectory. In the plot of the time-averaged MSD this effect will produce certain amplitude fluctuations, at a given lag time, between individual $\overline{\delta_i^2(t)}$. For scale-free continuous time random walk processes, due to the much more likely occurrence of extreme sojourn times, the amplitude fluctuations will be considerably more pronounced. Such amplitude scatter can be quantified in terms of the distribution $\phi(\xi)$, where the dimensionless variable $\xi = \overline{\delta^2(t)}/\langle\overline{\delta^2(t)}\rangle$ measures how much the time-averaged MSD $\overline{\delta^2(t)}$ deviates from the mean $\langle\overline{\delta^2(t)}\rangle$ [35, 36]. The amplitude scatter distribution $\phi(\xi)$ and its variance, the ergodicity breaking parameter $\mathrm{EB} = \langle\xi^2\rangle - 1$ have been calculated for a variety of processes [27, 35, 41, 42], and they encode distinct behaviours as functions of lag and measurement time for the different processes [27].

J. Stat. Mech. (2019) 114003

4. Single trajectory power spectra

The MSD and time-averaged MSD are standard measures for stochastic processes. However, there exists an alternative approach to quantify a diffusive dynamics, especially used in experimental data analysis, the power spectrum.

The standard textbook setting for spectral analyses is based on the so-called power spectral density (PSD) $\mu(f)$. To that end, the PSD is obtained by first calculating the Fourier transform of the individual trajectory $X(t)$, measured over the finite observation time T,

$$S(f,T) = \frac{1}{T}\left|\int_0^T \mathrm{e}^{\mathrm{i}ft}X(t)\mathrm{d}t\right|^2. \tag{12}$$

Here f denotes the frequency. The single-trajectory quantity $S(f,T)$ for finite observation times T naturally is a random variable, similar to our discussion of the time-averaged MSD above. The standard PSD is obtained from $S(f,T)$ as the ensemble average over all possible trajectories. With the additional long-measurement-time limit $T\to\infty$, the standard PSD yields in the form [48–50]

$$\begin{aligned}\mu(f) &= \lim_{T\to\infty}\frac{1}{T}\left\langle\left|\int_0^T \mathrm{e}^{\mathrm{i}ft}X(t)\mathrm{d}t\right|^2\right\rangle \\ &= \lim_{T\to\infty}\frac{1}{T}\int_0^T\int_0^T \cos(f[t_1-t_2])\langle X(t_1)X(t_2)\rangle \mathrm{d}t_1\mathrm{d}t_2,\end{aligned} \tag{13}$$

where angular brackets represent the statistical averaging and $\langle X(t_1)X(t_2)\rangle$ is the autocorrelation function of the process $X(t)$.

For the vastly growing number of single particle tracking experiments, the typical situation is that relatively few individual trajectories are garnered with a finite observation time T. Thus both the statistical averaging and the long time limit entering the definition (13) are problematic. As an alternative, practicable approach we therefore recently defined the single trajectory power spectral analysis based on expression (12) [49]. In general, the single-trajectory PSD (12) will not only be a function of the frequency f but also of the observation time T. In addition, fluctuations of $S(f,T)$ between results for individual trajectories will occur, even for normal Brownian motion [49]—in analogy to the amplitude fluctuations of the time-averaged MSD discussed above. While such trajectory-to-trajectory fluctuations may be mitigated by taking statistical averaging, we argue that important information may be drawn from these fluctuations—similar to the information from the amplitude scatter distribution $\phi(\xi)$ on the time-averaged MSD above.

The single trajectory power spectrum has so far been analysed for Brownian motion, fractional Brownian motion, and scaled Brownian motion [49–51]. In all these results the single-trajectory PSD (12) is proportional to the ensemble-averaged PSD (13), where depending on the process parameters the scaling with frequency exhibits the Brownian like $\simeq f^{-2}$ behaviour or a scaling exponent depending explicitly on the anomalous diffusion exponent α. Depending on the exact process the single-trajectory PSD (12) may feature an explicit, ageing dependence on the observation time T. Naturally,

J. Stat. Mech. (2019) 114003

see the discussion of the time-averaged MSD above, individual finite-T realisations will differ from each other by a random numerical factor in the single-trajectory PSD (12). The distribution of this amplitude was calculated analytically for Brownian motion and fractional Brownian motion [49, 50]. The shape of this distribution depends on whether one analyses the full three-dimensional motion, its two-dimensional projection typically measured by single particle tracking experiments, or the projection onto one dimension. Figure 2 demonstrates how well the experimentally observed behaviour matches the analytically predicted behaviour for four different systems in both subdiffusive and superdiffusive domains.

A special role is played by the coefficient of variation γ in the case of fractional Brownian motion, that can be described in terms of an overdamped Langevin equation driven by Gaussian but power-law correlated noise with noise autocorrelation $\xi(t)\xi(t') \sim \alpha(\alpha-1)K_\alpha|t-t'|^{\alpha-2}$ [27, 46]. For subdiffusion, the coefficient is negative, reflecting the antipersistent nature of the process, while for superdiffusion persistence is observed. As function of $\omega = fT$, γ has the unique value $\sqrt{2}$ in the zero frequency limit independent of the anomalous diffusion exponent α. In the large-ω limit, the result for γ reads

$$\gamma \sim \left[1 + \left(1 + c_\alpha \omega^{1-\alpha}\right)^{-2}\right]^{1/2}, \tag{14}$$

where $c_\alpha = \Gamma(1+\alpha)\sin(\pi\alpha/2)$. Remarkably, when we take $\omega \to \infty$ there only exist three different values of γ: $\sqrt{2}$ results for superdiffusion ($\alpha > 1$), $\sqrt{5}/2$ is obtained for normal Brownian motion ($\alpha = 1$), and 1 is the limiting value for subdiffusion ($\alpha < 1$) [50]. As shown from relatively few and short trajectories, γ allows one to distinguish the three regimes (superdiffusion, normal, diffusion, subdiffusion) even significantly away from the limit $\omega \to \infty$: it is sufficient to see whether the values depart from the Brownian one to show a tendency of growth or decrease [50].

Commonalities and differences between these Gaussian processes need careful analysis. In many respects the behaviour is the same for different processes when we look at one observable, for instance, the scaling exponent of the single-trajectory PSD, while the ageing dependence is different, etc. For the future a complete analysis of the single-trajectory PSD behaviour of a more exhaustive range of anomalous stochastic processes is called for, ultimately providing a very powerful tool to analyse measured time series, as an alternative to moment-based analyses.

5. Non-Gaussian diffusion processes: normal and anomalous

The central limit theorem is a cornerstone of statistical physics and mathematical statistics: according to this theorem the possible values of a properly scaled sum of independent, identically distributed (IID) random variables are governed by the normal Gaussian PDF in the limit of a large number of entries [52]. This convergence is strong in the sense that it is independent of the exact form of the distribution of the component IID variables, if only they are characterised by a finite variance. An outstanding example for this mathematical statement is the convergence of the position distribution of a normal random walk to the Gaussian (2) [53]. In particular, this solution (2) of

J. Stat. Mech. (2019) 114003

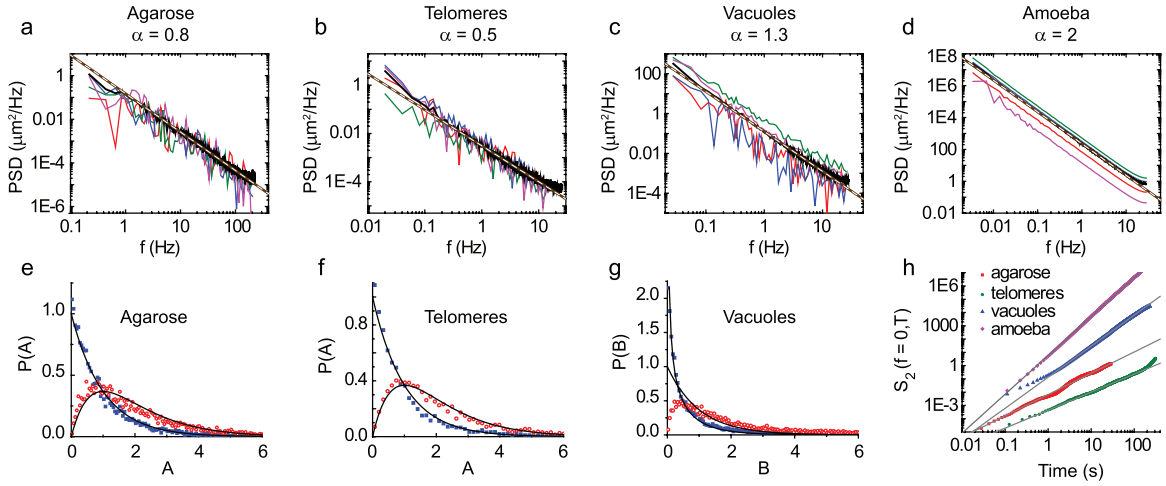

Figure 2. Power spectral analysis of experimental data sets, taken from [50]. (a)–(d) Single-trajectory PSD of representative trajectories along with the ensemble-averaged PSD for telomeres in the nucleus of HeLa cells, 50 nm nanoparticles in 1.5% agarose gel, intracellular vacuoles within amoeba, and the motion of amoeba. The anomalous diffusion exponent in the panels indicates sub- and superdiffusive dynamics. The dashed thick lines show the power-laws $1/f^{1.49}$ for panel (a), $1/f^{1.76}$ for panel (b) and $1/f^2$ for panels (c) and (d). In each case, the PSDs of four trajectories are presented (log-sampled with a factor 1.1 for clarity) together with the ensemble-averaged PSD (thicker black lines, $n = 19, 20, 50,$ and 4 trajectories for telomeres, nanoparticles, vacuoles, and amoeba, respectively). (e)–(g) Amplitude distribution of the PSD for one and two dimensions. (h) Zero frequency PSD, showing the ageing dependence mentioned in the text. For more details see [50].

the diffusion equation features the scaling variable $|\mathbf{r}^2|/t$, giving rise to the Brownian (Fickian) MSD (1) with its linear time dependence.

Often, the observation of an MSD of the linear form (1) is taken to imply that we are dealing with normal Brownian motion, and that the PDF of the process therefore has to be the Gaussian (2). A number of recent data from a range of different systems demonstrate, however, that a linear MSD (1) can come along with highly non-Gaussian forms of the PDF $P(\mathbf{r}, t)$ [54, 55]. For instance, the motion of biomacromolecules, proteins and viruses along lipid tubes and through actin networks [54, 55], as well as along membranes and inside colloidal suspension [56] and colloidal nanoparticles adsorbed at fluid interfaces [57–59] show this 'Brownian yet non-Gaussian' behaviour. A similar combination of the law (1) with non-Gaussian properties was observed in ecological processes of organism movement and dispersal [60, 61]. There exist also processes, that are Brownian but non-Gaussian in certain time windows of their dynamics observed for the dynamics of disordered solids, such as glasses and supercooled liquids [62–64] as well as for interfacial dynamics [65, 66].

To see how a non-Gaussian PDF may arise while the MSD is linear in time, consider a mixture of diffusing particles with non-identical diffusivities D. An example could be commercial tracer beads that always have a certain size distribution due to imperfections in the manufacturing process. Indeed, already Jean Perrin faced this problem in his early single particle tracking experiments. While each particle is Brownian and, for

J. Stat. Mech. (2019) 114003

its own D value, characterised by a Gaussian $P(\mathbf{r},t|D)$[1], if we measure the PDF for the entire 'ensemble' of the non-identical particles the result will be the average

$$P(\mathbf{r},t) = \int_0^\infty p(D)P(\mathbf{r},t|D)dD. \tag{15}$$

Here $p(D)$ quantifies the distribution of diffusivities among the tracer particles. In fact, the formulation (15) is identical to the concept of superstatistics formulated by Beck and Cohen [67], see also [68]. Their original scenario for relation (15) was that individual particles move in different regions characterised by different D. In this scenario, of course, each particle will eventually reach the border of its seed region and move to a region with a different D, and $p(D)$ would become explicitly time dependent. However, in the superstatistical formulation (15) $p(D)$ is time independent. We note that the superstatistical formulation was also achieved starting from a stochastic Langevin equation [69]. Moreover, a similar, random-parameter formulation of diffusion processes is given by the concept of generalised grey Brownian motion (ggBm) [70, 71].

The first results in [54, 55] of the non-Gaussian distribution $P(\mathbf{r},t)$ were the exponential or 'Laplace' distribution. One can show [72] that this form of $P(\mathbf{r},t)$ uniquely emerges from an exponential distribution $p(D)$. More complicated forms of $p(D)$ are often found in terms of generalised gamma distributions, as observed in [60], or stretched Gaussian shapes [61]. Superstatistical and ggBm formulations based on the generalised gamma distribution were introduced in [60, 71, 73].

In its formulation above superstatistics cannot account for the crossover to a Gaussian PDF at times longer than some correlation time observed in some of the experiments [54, 55]. This was achieved by Chubinsky and Slater in their model of 'diffusing diffusivity' [74]. This approach was further developed by Jain and Sebastian [75], Chechkin *et al* [72], Tyagi and Cherayil [76], Lanoiselée and Grebenkov [77], as well as Sposini *et al* [71]. The basic idea by Chubinsky and Slater is that the diffusion coefficient in a single trajectory is a stochastic quantity, changing its value perpetually along the trajectory of the tracer particle. Physically, this is a simplified picture for a particle moving in a heterogeneous environment, imposing continuous changes in the particle mobility along its path. Concretely, in a minimal formulation of the diffusing diffusivity model, this motion can be captured by the set of coupled stochastic equations [72]

$$\frac{\mathrm{d}}{\mathrm{d}t}\mathbf{r}(t) = \sqrt{2D(t)}\boldsymbol{\xi}(t), \tag{16a}$$

$$D(t) = \mathbf{Y}^2(t), \tag{16b}$$

$$\frac{\mathrm{d}}{\mathrm{d}t}\mathbf{Y}(t) = -\frac{1}{\tau}\mathbf{Y} + \sigma\boldsymbol{\eta}(t). \tag{16c}$$

Here expression (16*a*) is the Langevin equation for a a particle driven by the white Gaussian noise $\boldsymbol{\xi}(t)$. However, the associated amplitude contains the explicitly

[1] We use the explicit conditional probability notation to indicate the D-dependence of the PDF.

J. Stat. Mech. (2019) 114003

time-dependent diffusion coefficient. This property is specified by equation (16*b*), that maps D onto the squared auxiliary quantity $\mathbf{Y}$ thus guaranteeing positivity of the diffusivity, and (16*c*). The latter, stochastic equation describes the time evolution of $\mathbf{Y}$ driven by another white Gaussian noise $\boldsymbol{\eta}(t)$. However, in contrast to equation (16*a*), the motion of $\mathbf{Y}$ is confined and thus will relax to equilibrium above the crossover time τ. In fact, equation (16*c*) is the famed Ornstein–Uhlenbeck process [53]. In the analysis of [72] it was shown that this formulation of the diffusing diffusivity model at short times reproduces the superstatistical approach, while at times longer than the correlation time τ of the auxiliary $\mathbf{Y}$ process a crossover occurs to a Gaussian PDF characterised by a single, effective diffusion coefficient. This crossover can be conveniently characterised by the kurtosis $K = \langle \mathbf{r}^4(t)\rangle / \langle \mathbf{r}^2(t)\rangle^2$ [72]. More technically, the formulation in terms of the minimal model (16*a*) to (16*c*) corresponds to a subordination approach, which is helpful in obtaining exact analytical results and in formulating a two-variable Fokker–Planck equation for the diffusing diffusivity process [72]. We note that the first-passage behaviour of the diffusing diffusivity model was analysed in [78, 79].

In figure 3 we show the behaviour encoded in the minimal diffusing diffusivity model (16*a*) to (16*c*). The three panels respectively show the crossover from an initial Laplace distribution with exponential tails to a Gaussian (left), the fact that the MSD of the process always is linear in time with a constant coefficient (middle), and the crossover behaviour measured by the kurtosis (right). This behaviour is characteristic for an equilibrium condition of the auxiliary variable $\mathbf{Y}$. The more general situation for a non-equilibrium initial condition with crossovers in the associated MSD is analysed in [71]. We remark that the diffusing diffusivity model developed here is closely related to the Cox–Ingersoll–Ross (CIR) model for monetary returns which is widely used in financial mathematics [80].

What about anomalous diffusion processes? Fractional Brownian motion (FBM) and fractional Langevin equation (FLE) motion[2] are both processes driven by power-law correlated (fractional) Gaussian noise, and are therefore characterised by a Gaussian PDF. For the motion of constituent molecules in membrane systems it was shown in a supercomputing study that the dynamics is Gaussian and driven by fractional Gaussian noise [82], however, when the membrane is crowded by large embedded proteins, strongly non-Gaussian behaviour with intermittent diffusivity occurs [83]. In single particle tracking experiments in heterogeneous membranes an exponential distribution of the diffusivity was shown to result, along with a Laplace distribution of the PDF [84]. Finally we mention the study [85] of tracer diffusion in bacteria and yeast cells, where a Laplace-PDF and exponential diffusivity distribution were presented and motivated by a superstatistical FBM approach. Similarly to this approach, a superstatistical generalised Langevin equation model was studied by Beck and van der Straeten [86], while a more general approach for a superstatistical generalised Langevin equation was introduced by Ślęzak [87] in which it was shown that the distribution of the position variable is characterised by a relaxation from a Gaussian to a non-Gaussian distribution.

[2] The FLE is a version of the generalised Langevin equation with a power-law friction kernel [47, 81].

J. Stat. Mech. (2019) 114003

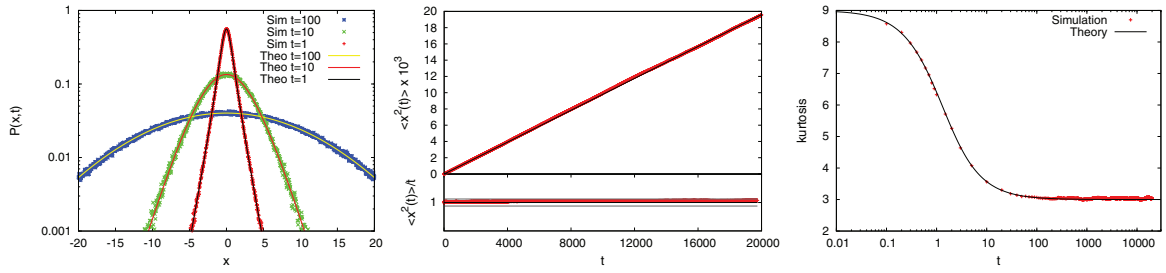

Figure 3. Behaviour of the minimal model for diffusing diffusivity, equations (16*a*) to (16*c*) in the one-dimensional case, figures reproduced from [72]. Left: PDF $P(x,t)$ at different times, demonstrating the crossover from the short-time exponential to the long-time Gaussian form, shown here for simulations and the theoretical result. Middle: the MSD shows a linear behaviour with constant coefficient, as seen in the lower panel, in which the MSD/t is shown. Right: the kurtosis crosses over from the value $K = 9$ for a one-dimensional Laplace distribution to the value $K = 3$ for a one-dimensional Gaussian; the crossover time corresponds to the preset value $\tau = 1$.

Random parameter diffusion models are very actively studied, and we can here only give a limited overview. Apart from the developments sketched above we mention the study by Cherstvy *et al* [88] in which scaled Brownian motion for massive and massless particles was analysed for a Rayleigh distribution of the diffusion coefficient. Stylianidou *et al* [89] show that in a random barrier model anomalous diffusion with exponential-like step size distribution and anticorrelations emerge, similar to the behaviour measured by Lampo *et al* [85], with a crossover to Brownian and Gaussian behaviour at sufficiently long times. Sokolov *et al* compare the diffusing diffusivity model with the emerging dynamics when the quenched nature of a disordered environment is explicitly taken into account [90]. Moreover, we mention a study by Barkai and Burov [91], in which the authors use extreme value statistic arguments to derive a robust exponential shape of the displacement PDF. Finally, in a recent work Ślęzak *et al* [92] show that random coefficient autoregressive processes of the ARMA type can be used to describe Brownian yet non-Gaussian processes, and thus connect the world of physics of such dynamics with the world of time series analysis.

We close this section with the remark that continuous time random walk processes with scale-free waiting times as well as heterogeneous diffusion processes inherently have a non-Gaussian distribution [26, 27, 42], as does diffusion on fractal supports such as percolation clusters close to criticality [93]. Finally, a completely different mechanism for non-Gaussianity is currently being explored. Namely, while normal Brownian motion initiated right next to a reflecting boundary will develop as a half-Gaussian, fractional Brownian motion with its correlated increments shows pronounced deviations from the Gaussian form in the vicinity of the boundary, and does also not converge to a constant distribution in a finite box domain [94].

J. Stat. Mech. (2019) 114003

6. Conclusions

Despite its relatively long history and the existence of numerous textbooks the theory of Brownian motion is still far from complete. Less surprisingly, anomalous stochastic processes are still actively studied. We here mentioned some of the recent developments, including the calculation of the full distributions of first-passage times in generic confined volumes and for targets with finite reactivity, the theory of time-averaged moments and the feature of non-ergodicity and ageing, the single-trajectory power spectral density, and the emergence of non-Gaussian distributions in heterogeneous media. These developments are motivated by novel experimental techniques, for instance, superresolution microscopy and/or single particle tracking in complex environments such as living biological cells. In this endeavour, however, theory also feeds back to experiment. A prime example is the analysis of Perrin that would not have been possible without the theories by Einstein, Smoluchowski, and Langevin. The recent mathematical results for stochastic processes presented here will allow experimentalists to compare their observations with these predictions and help them to extract the physical parameters and identify the underlying stochastic mechanisms.

One of the major lessons coming from the current theoretical analysis of stochastic processes is that, instead of aiming at producing smooth curves in terms of averaging over as many particles as possible, valuable information can indeed be gained from the fluctuations of the measured quantities. Thus, for the amplitude scatter distribution $\phi(\xi)$ of the time-averaged MSD distinct patterns emerge for different stochastic processes, helping in distinguishing these physical mechanisms when analysing data. Similarly the lag and observation time dependence of the ergodicity breaking parameter EB has a similar diagnostic rôle. Amplitude fluctuations have also been calculated for the single-trajectory power spectral density. Once this property is known for a larger class of stochastic processes, these fluctuations will similarly act as a criterion for model selection. To acknowledge the presence of strong fluctuations is also important given our discussion of first-passage times and their defocusing.

Data analysis is becoming ever more relevant as more and higher quality data are being obtained. As we saw, there exist numerous, qualitatively different anomalous stochastic processes. To learn about the physics of a system, the exact underlying stochastic mechanism needs to be identified, along with reliable values for the systems parameters. This is currently being investigated, using different approaches. We here mention Bayesian based maximum likelihood methods tailored for diffusive systems [95], as well as machine learning suites [96]. Considerable advances in this field over the coming years are to be expected. In parallel, theorists are developing new tools for the data analysis, such as the moment or power spectral analysis mentioned here, or other methods such as the p-variation technique [97], apparent diffusivity distributions [98], covariance-based estimators [99], or the codifference, that is able to detect ergodicity breaking and non-Gaussianity in measured data [100].

The exploration of stochastic processes is still going strong, revealing new and relevant theoretical results allowing experimentalists to focus their studies, while concurrently new types of experiments and ever improving precision, resolution, and sheer amounts of measured data pose new challenges for the theoretical analysis.

J. Stat. Mech. (2019) 114003

Acknowledgments

RM acknowledges funding from Deutsche Forschungsgemeinschaft (DFG code ME 1535/7-1) as well as from the Foundation for Polish Science (Fundacja na rzecz Nauki Polskiej) within an Alexander von Humboldt Polish Honorary Research Scholarship.

References

[1] Brown R 1828 *Phil. Mag.* **4** 161
Brown R 1828 *Ann. Phys. Chem.* **14** 294
[2] Einstein A 1905 *Ann. Phys., Lpz.* **322** 549
[3] Sutherland W 1905 *Phil. Mag.* **9** 781
[4] von Smoluchowski M 1906 *Ann. Phys., Lpz.* **21** 756
[5] Langevin P 1908 *C. R. Acad. Sci., Paris* **146** 530
[6] Pearson K 1905 *Nature* **72** 294
Rayleigh 1905 *Nature* **72** 318
[7] Perrin J 1908 *C. R.* **146** 967
Perrin J 1909 *Ann. Chim. Phys.* **18** 5
[8] Nordlund I 1914 *Z. Phys. Chem.* **87** 40
[9] Kappler E 1931 *Ann. Phys., Lpz.* **11** 233
[10] Moerner W E and Orrit M 1999 *Science* **238** 1670
Saxton M J and Jacobsen K 1997 *Ann. Rev. Biophys. Biomol. Struct.* **26** 373
Xie X S, Choi P J, Li G-W, Lee N K and Lia G 2008 *Annu. Rev. Biophys.* **37** 417
Bräuchle C, Lamb D C and Michaelis J 2012 *Single Particle Tracking and Single Molecule Energy Transfer* (New York: Wiley)
[11] Nørregaard K, Metzler R, Ritter C M, Berg-Sørensen K and Oddershede L B 2017 *Chem. Rev.* **117** 4342
Höfling F and Franosch T 2013 *Rep. Prog. Phys.* **76** 046602
[12] di Rienzo C *et al* 2014 *Nat. Commun.* **5** 5891
[13] Metzler R, Jeon J-H and Cherstvy A G 2016 *Biochimica et Biophysica Acta—Biomembr.* **1858** 2451
[14] Redner S 2001 *A Guide to First Passage Processes* (Cambridge: Cambridge University Press)
[15] Koren T, Lomholt M A, Chechkin A V, Klafter J and Metzler R 2007 *Phys. Rev. Lett.* **99** 160602
Chechkin A V, Metzler R, Klafter J, Gonchar V Yu and Tanatarov L V 2003 *J Phys.* A **36** L537
Padash A, Chechkin A V, Dybiec B, Pavlyukevich I, Shokri B and Metzler R 2019 *J Phys.* A **52** 454004
Palyulin V V, Blackburn G, Lomholt M A, Watkins N W, Metzler R, Klages R and Chechkin A V 2019 *J. Phys.* **21** 103028
[16] Bénichou O and Voituriez R 2014 *Phys. Rep.* **539** 225
Condamin S, Bénichou O, Tejedor V, Voituriez R and Klafter J 2007 *Nature* **450** 77
Bénichou O, Chevalier C, Klafter J, Meyer B and Voituriez R 2010 *Nat. Chem.* **2** 472–7
[17] Mejía-Monasterio C, Oshanin G and Schehr G 2011 *J. Stat. Mech.* P06022
Mattos T, Mejía-Monasterio C, Metzler R and Oshanin G 2012 *Phys. Rev.* E **86** 031143
[18] Kolesov G, Wunderlich Z, Laikova O N, Gelfand M S and Mirny L A 2007 *Proc. Natl Acad. Sci. USA* **104** 13948
Pulkkinen O and Metzler R 2013 *Phys. Rev. Lett.* **110** 198101
[19] Bauer M, Rasmussen E S, Lomholt M A and Metzler R 2015 *Sci. Rep.* **5** 10072
[20] Yu J, Xiao J, Ren X, Lao K and Xie X S 2006 *Science* **311** 1600
[21] Godec A and Metzler R 2016 *Phys. Rev.* X **6** 041037
Godec A and Metzler R 2016 *Sci. Rep.* **6** 20349
[22] Grebenkov D S, Metzler R and Oshanin G 2018 *Phys. Chem. Chem. Phys.* **20** 16393
[23] Grebenkov D, Metzler R and Oshanin G 2018 *Commun. Chem.* **1** 96
[24] Collins F C and Kimball G E 1949 *J. Colloid Sci.* **4** 425
[25] Bouchaud J-P and Georges A 1990 *Phys. Rep.* **195** 127
[26] Metzler R and Klafter J 2000 *Phys. Rep.* **339** 1
[27] Metzler R, Jeon J-H, Cherstvy A G and Barkai E 2014 *Phys. Chem. Chem. Phys.* **16** 24128
[28] Scher H and Montroll E W 1975 *Phys. Rev.* B **12** 2455
[29] Schubert M, Preis E, Blakesley J C, Pingel P, Scherf U and Neher D 2013 *Phys. Rev.* B **87** 024203
[30] Edery Y, Scher H, Guadagnini A and Berkowitz B 2014 *Water Res. Res.* **50** 1490
Berkowitz B, Scher H and Silliman S E 2000 *Water Res. Res.* **36** 149
Schumer R, Benson D A, Meerschaert M and Baeumer B 2003 *Water Res. Res.* **39** 13

J. Stat. Mech. (2019) 114003

[31] Weiss M, Elsner M, Kartberg F and Nilsson T 2004 *Biophys. J.* **87** 3518
Golding I and Cox E C 2006 *Phys. Rev. Lett.* **96** 098102
Bronstein I, Israel Y, Kepten E, Mai S, Shav-Tal Y, Barkai E and Garini Y 2009 *Phys. Rev. Lett.* **103** 018102
Guigas G, Kalla C and Weiss M 2007 *Biophys. J.* **93** 316
Weber S C, Spakowitz A J and Theriot J A 2010 *Phys. Rev. Lett.* **104** 238102
Jeon J-H, Tejedor V, Burov S, Barkai E, Selhuber-Unkel C, Berg-Sørensen K, Oddershede L and Metzler R 2011 *Phys. Rev. Lett.* **106** 048103
Burnecki K, Kepten E, Janczura J, Bronshtein I, Garini Y and Weron A 2012 *Biophys. J.* **103** 1839
Tabei S M, Burov S, Kim H Y, Kuznetsov A, Huynh T, Jureller J, Philipson L H, Dinner A R and Scherer N F 2013 *Proc. Natl Acad. Sci. USA* **110** 4911
[32] Solomon T H, Weeks E R and Swinney H L 1993 *Phys. Rev. Lett.* **71** 3975
Zaslavsky G M 2002 *Phys. Rep.* **371** 461
Richardson L F 1926 *Proc. R. Soc.* A **110** 709
[33] Caspi A, Granek R and Elbaum M 2000 *Phys. Rev. Lett.* **85** 5655
Seisenberger G, Ried M U, Endreß T, Büning H, Hallek M and Bräuchle C 2001 *Science* **294** 1929
Robert D, Nguyen T H, Gallet F and Wilhelm C 2010 *PLoS One* **4** e10046
Reverey J F, Jeon J-H, Leippe M, Metzler R and Selhuber-Unkel C 2015 *Sci. Rep.* **5** 11690
[34] Tejedor V, Benichou O, Voituriez R, Jungmann R, Simmel F, Selhuber-Unkel C, Oddershede L and Metzler R 2010 *Biophys. J.* **98** 1364
[35] He Y, Burov S, Metzler R and Barkai E 2008 *Phys. Rev. Lett.* **101** 058101
[36] Barkai E, Garini Y and Metzler R 2012 *Phys. Today* **65** 29
[37] Weigel A V, Simon B, Tamkun M M and Krapf D 2011 *Proc. Natl Acad. Sci. USA* **108** 6438
Weigel A V, Tamkun M M and Krapf D 2013 *Proc. Natl Acad. Sci. USA* **110** E4591
[38] Schulz J H P, Barkai E and Metzler R 2013 *Phys. Rev. Lett.* **110** 020602
Schulz J H P, Barkai E and Metzler R 2014 *Phys. Rev.* X **4** 011028
[39] Barkai E 2003 *Phys. Rev. Lett.* **90** 104101
Barkai E and Cheng Y C 2003 *J. Chem. Phys.* **118** 6167
[40] Mardoukhi Y, Jeon J-H and Metzler R 2015 *Phys. Chem. Chem. Phys.* **17** 30134
Mardoukhi Y, Jeon J-H, Chechkin A V and Metzler R 2018 *Phys. Chem. Chem. Phys.* **20** 20427
[41] Lim S C and Muniandy S V 2002 *Phys. Rev.* E **66** 021114
Fuliński A 2013 *J. Chem. Phys.* **138** 021101
Jeon J-H, Chechkin A V and Metzler R 2014 *Phys. Chem. Chem. Phys.* **16** 15811
[42] Cherstvy A G, Chechkin A V and Metzler R 2013 *New J. Phys.* **15** 083039
Cherstvy A G and Metzler R 2014 *Phys. Rev.* E **90** 012134
Cherstvy A G, Chechkin A V and Metzler R 2014 *J. Phys. A: Math. Theor.* A **47** 485002
[43] Cherstvy A G and Metzler R 2013 *Phys. Chem. Chem. Phys.* **15** 20220
[44] Krüsemann H, Godec A and Metzler R 2014 *Phys. Rev.* E **89** 040101
Krüsemann H, Godec A and Metzler R 2015 *J. Phys. A: Math. Theor.* A **48** 285001
Krüsemann H, Schwarzl R and Metzler R 2016 *Transp. Porous Media* **115** 327
[45] Mandelbrot B B and van Ness J W 1968 *SIAM Rev.* **10** 422
[46] Deng W and Barkai E 2009 *Phys. Rev.* E **79** 011112
Schwarzl M, Godec A and Metzler R 2017 *Sci. Rep.* **7** 3878
[47] Goychuk I 2009 *Phys. Rev.* E **80** 046125
Goychuk I 2012 *Adv. Chem. Phys.* **150** 187
[48] Norton M P and Karczub D G 2003 *Fundamentals of Noise and Vibration Analysis for Engineers* (Cambridge: Cambridge University Press)
[49] Krapf D, Marinari E, Metzler R, Oshanin G, Xu X and Squarcini S 2018 *New J. Phys.* **20** 023029
[50] Krapf D, Lukat N, Marinari E, Metzler R, Oshanin G, Selhuber-Unkel C, Squarcini A, Stadler L, Weiss M and Xu X 2019 *Phys. Rev.* X **9** 011019
[51] Sposini V, Metzler R and Oshanin G 2019 *New J. Phys.* **21** 073043
[52] Feller W 1970 *An Introduction to Probability Theory and its Application* (New York: Wiley)
[53] van Kampen N 1981 *Stochastic Processes in Physics and Chemistry* (Amsterdam: North-Holland)
[54] Wang B, Kuo J, Bae S C and Granick S 2012 *Nat. Mater.* **11** 481
[55] Wang B, Antony S M, Bae S C and Granick S 2009 *Proc. Natl Acad. Sci. USA* **106** 15160
[56] Leptos K C, Guasto J S, Gollub J P, Pesci A I and Goldstein R E 2009 *Phys. Rev. Lett.* **103** 198103
[57] Xue C, Zheng X, Chen K, Tian Y and Hu G 2016 *J. Phys. Chem. Lett.* **7** 514
[58] Wang D, Hu R, Skaug M J and Schwartz D 2015 *J. Phys. Chem. Lett.* **6** 54
[59] Dutta S and Chakrabarti J 2016 *Europhys. Lett.* **116** 38001
[60] Hapca S, Crawford J W and Young I M 2009 *J. R. Soc. Interface* **6** 111

J. Stat. Mech. (2019) 114003

[61] Cherstvy A G, Günther O, Beta C and Metzler R 2018 *Phys. Chem. Chem. Phys.* **20** 23034
[62] Kob W and Andersen H C 1995 *Phys. Rev.* E **51** 4626
[63] Chaudhuri P, Berthier L and Kob W 2007 *Phys. Rev. Lett.* **99** 060604
[64] Roldàn-Vargas S, Rovigatti L and Sciortino F 2017 *Soft Matter* **13** 514
[65] Samanta N and Chakrabarti R 2016 *Soft Matter* **12** 8563
[66] Skaug M J, Wang L, Ding Y and Schwartz D K 2015 *ACS Nano* **9** 2148
[67] Beck C and Cohen E D B 2003 *Physica* A **322** 267
[68] Beck C 2006 *Prog. Theor. Phys. Suppl.* **162** 29
[69] van der Straeten E and Beck C 2009 *Phys. Rev.* E **80** 036108
[70] Mura A, Taqqu M S and Mainardi F 2008 *Physica* A **387** 5033
Mura A and Pagnini G 2008 *J. Phys. A: Math. Theor.* **41** 285003
Mura A and Mainardi F 2009 *Int. Transfer Spectrosc. Funct.* **20** 185
Molina-García D, Pham T M, Paradisi P and Pagnini G 2016 *Phys. Rev.* E **94** 052147
[71] Sposini V, Chechkin A V, Seno F, Pagnini G and Metzler R 2018 *New J. Phys.* **20** 043044
[72] Chechkin A V, Seno F, Metzler R and Sokolov I M 2017 *Phys. Rev.* X **7** 021002
[73] Beck C 2006 *Physica* A **365** 96
[74] Chubynsky M V and Slater G W 2014 *Phys. Rev. Lett.* **113** 098302
[75] Jain R and Sebastian K L 2016 *J. Phys. Chem.* B **120** 3988
Jain R and Sebastian K L 2017 *J. Chem. Sci.* **129** 929
[76] Tyagi N and Cherayil B J 2017 *J. Phys. Chem.* B **121** 7204
[77] Lanoiselée Y and Grebenkov D 2018 *J. Phys. A: Math. Theor.* A **51** 145602
[78] Lanoiselée Y, Moutal N and Grebenkov D 2018 *Nat. Commun.* **9** 4398
[79] Sposini V, Chechkin A V and Metzler R 2019 *J. Phys. A: Math. Theor.* A **52** 04LT01
[80] Fouqué J-P, Papanicolaou G and Sircar K R 2000 *Derivatives in Financial Markets with Stochastic Volatility* (Cambridge: Cambridge University Press)
Cox J C, Ingersoll J E and Ross S A 1985 *Econometrica* **53** 385
See also Heston S L 1993 *Rev. Financ. Stud.* **6** 327
[81] Lutz E 2001 *Phys. Rev.* E **64** 051106
[82] Jeon J-H, Monne H M-S, Javanainen M and Metzler R 2012 *Phys. Rev. Lett.* **109** 188103
Kneller G R, Baczynski K and Pasenkiewicz-Gierula M 2011 *J. Chem. Phys.* **135** 141105
[83] Jeon J-H, Javanainen M, Martinez-Seara H, Metzler R and Vattulainen I 2016 *Phys. Rev.* X **6** 021006
[84] He W, Song H, Su Y, Geng L, Ackerson B J, Peng H B and Tong P 2016 *Nat. Commun.* **7** 11701
[85] Lampo T, Stylianido S, Backlund M P, Wiggins P A and Spakowitz A J 2017 *Biophys. J.* **112** 532
[86] van der Straeten E and Beck C 2011 *Physica* A **390** 951
[87] Ślęzak J, Metzler R and Magdziarz M 2018 *New J. Phys.* **20** 023026
[88] Cherstvy A G and Metzler R 2016 *Phys. Chem. Chem. Phys.* **18** 23840
[89] Stylianido S, Lampo T J, Spakowitz A J and Wiggins P A 2018 *Phys. Rev.* E **97** 062410
[90] Sokolov I M and Chechkin A V 2018 (arXiv:1810.02605)
[91] Barkai E and Burov S 2019 (arXiv:1908.02916)
[92] Ślęzak J, Burnecki K and Metzler R 2019 *New J. Phys.* **21** 073056
[93] Havlin S and Ben-Avraham D 1987 *Adv. Phys.* **36** 695
[94] Wada A H O and Vojta T 2018 *Phys. Rev.* E **97** 020102
Guggenberger T, Pagnini G, Vojta T and Metzler R 2019 *New J. Phys.* **21** 022002
[95] Robson A, Burrage K and Leake M C 2012 *Phil. Trans. R. Soc.* B **368** 20120029
Krog J and Lomholt M A 2017 *Phys. Rev.* E **96** 062106
Thapa S, Lomholt M A, Krog J, Cherstvy A G and Metzler R 2018 *Phys. Chem. Chem. Phys.* **20** 29018
Cherstvy A G, Thapa S, Wagner C E and Metzler R 2019 *Soft Matter* **15** 2526
[96] Granik N, Nehme E, Weiss L E, Levin M, Chein M, Perlson E, Roichman Y and Shechtman Y 2019 *Biophys. J.* **117** 185
Muñoz-Gil G, Garcia-March M A, Manzo C, Martín-Guerrero J D and Lewenstein M 2019 (arXiv:1903.02850)
[97] Magdziarz M, Weron A, Burnecki K and Klafter J 2009 *Phys. Rev. Lett.* **103** 180602
Magdziarz M and Klafter J 2010 *Phys. Rev.* E **82** 011129
[98] Heidernaetsch M, Bauer M and Radons G 2013 *J. Chem. Phys.* **139** 184105
[99] Vestergaard C L, Blainey P C and Flyvbjerg H 2014 *Phys. Rev.* E **89** 022726
[100] Ślęzak J, Metzler R and Magdziarz M 2019 *New J. Phys.* **21** 053008

J. Stat. Mech. (2019) 114003